JOURNAL OF APPLIED PHYSICS **113**, 183910 (2013)

Pressure induced para-antiferromagnetic switching in $BiFeO_3$–$PbTiO_3$ as determined using *in-situ* neutron diffraction

Tim P. Comyn,[1] Tim Stevenson,[1] Maisoon Al-Jawad,[2] William G. Marshall,[3] Ronald I. Smith,[3] Julia Herrero-Albillos,[4] Robert Cywinski,[5] and Andrew J. Bell[1]
[1]*Institute for Materials Research, University of Leeds, Leeds LS2 9JT, United Kingdom*
[2]*Dental Physical Sciences Group, Queen Mary, University of London, London E1 4NS, United Kingdom*
[3]*ISIS Facility, STFC Rutherford Appleton Laboratory, Harwell Science & Innovation Campus, Chilton, Didcot, Oxfordshire OX11 OQX, United Kingdom*
[4]*Helmholtz-Zentrum Berlin für Materialien und Energie GmbH, Albert-Einstein-Str. 15, 12489 Berlin, Germany*
[5]*School of Applied Sciences, University of Huddersfield, Huddersfield HD1 3DH, United Kingdom*

(Received 4 December 2012; accepted 24 April 2013; published online 13 May 2013)

$BiFeO_3$–$PbTiO_3$ exhibits both ferroelectric and antiferromagnetic order, depending on the composition. Moderate hydrostatic pressures have been used at room temperature to transform the crystallographic phase from P4mm to R3c for the compositions $0.7BiFeO_3$–$0.3PbTiO_3$ and $0.65BiFeO_3$–$0.35PbTiO_3$, as determined using *in-situ* neutron diffraction. Using Rietveld refinements, the resultant data showed that, for both compositions, a transformation from para- to G-type antiferromagnetic order accompanied the structural transition. The transformation occurred over the range 0.4–0.77 and 0.67–0.88 GPa for $0.7BiFeO_3$–$0.3PbTiO_3$ and $0.65BiFeO_3$–$0.35PbTiO_3$, respectively; at intermediate pressures, a mixture of P4mm and R3c phases were evident. These pressures are far lower than required to induce a phase transition in either the $BiFeO_3$ or $PbTiO_3$ end members. The driving force for this pressure induced first order phase transition is a significant difference in volume between the two phases, P4mm > R3c of 4%-5%, at ambient pressure. Upon removal of the pressure, $0.65BiFeO_3$–$0.35PbTiO_3$ returned to the paramagnetic tetragonal state, whereas in $0.7BiFeO_3$–$0.3PbTiO_3$ antiferromagnetic ordering persisted, and the structural phase remained rhombohedral. Using conventional laboratory x-ray diffraction with a hot-stage, the phase readily reverted back to a tetragonal phase, at temperatures between 100 and 310 °C for $0.7BiFeO_3$–$0.3PbTiO_3$, far lower than the ferroelectric Curie point for this composition of 632 °C. To our knowledge, the reported pressure induced para- to antiferromagnetic transition is unique in the literature. © *2013 AIP Publishing LLC*. [http://dx.doi.org/10.1063/1.4804322]

I. INTRODUCTION

$BiFeO_3$ is a multiferroic material, displaying both antiferromagnetic and ferroelectric ordering at room temperature.[1–3] Such materials offer potential in a range of applications (i.e., memory devices and sensors), and the possibility of magnetoelectric coupling, that is control of magnetization with electrical stimulus and vice versa. A solid solution may be formed with the ferroelectric $PbTiO_3$, to generate $xBiFeO_3$–$(1-x)PbTiO_3$, which is also multiferroic for $0.3 \leq x \leq 1$ at room temperature.[4] The system $xBiFeO_3$–$(1-x)PbTiO_3$ has been shown to consist of a mixture of rhombohedral (R3c) and tetragonal (P4mm) phases for $0.6 \leq x \leq 0.8$.[5] An enhancement in both ferroelectric and piezoelectric properties is observed for $x = 0.7$, compared to neighboring compositions.[6] Extremely high micro-strains are evident in these mixed phase materials due to the radically different molar volumes of each phase[7] and the large spontaneous strain, (c-a)/a,[8] for the P4mm symmetry, of 0.187. For hot-pressed pellets of $0.72BiFeO_3$–$0.28PbTiO_3$, Smith[7] observed the volume of the tetragonal unit cell to be ca. 5% larger than that of the rhombohedral cell (primitive volume = R3c/6). We have recently confirmed the same using neutron diffraction experiments for the composition $0.7BiFeO_3$–$0.3PbTiO_3$;[9] in addition, we have shown that depending on the specific processing conditions, the proportions of R3c and P4mm can be tailored, consisting of predominantly R3c for a sintered ceramic and P4mm in powder form. Recent work also suggests the possibility of monoclinic rather than rhombohedral symmetry in the composition $0.73BiFeO_3$–$0.27PbTiO_3$.[10]

Studies of the composition $0.9BiFeO_3$–$0.1PbTiO_3$ using neutron diffraction as a function of temperature show correlation between the Néel temperature and the maximum in spontaneous strain ($\tan(90-\alpha)$, for the primitive rhombohedral phase, where α is the rhombohedral angle) in a significant deviation from typical Landau behavior.[11] This strongly points to a coupling between the ferroic orders.

Pressure induced phase transitions have been observed in a gamut of ferroelectric, antiferroelectric, and multiferroic materials, using neutron/synchrotron diffraction, magnetic and electrical measurements in addition to Raman and Mössbauer techniques.

The application of hydrostatic pressure on $BiFeO_3$ has been studied by a number of groups. Haumont[12,13] and Pashkin[14] used Raman spectroscopy, far infrared and synchrotron diffraction measurements to show the presence of two structural phase transitions (rhombohedral—orthorhombic(1)—orthorhombic(2)) at ranges of between 2.5–3.5 GPa and

7.5–10 GPa. Gavriliuk[15] observed a transformation from antiferromagnetic to a non-magnetic state at a far higher pressure of 47 GPa for $BiFeO_3$ powders using Mössbauer spectroscopy. Belik[16] observed phase transitions at 4 and 7 GPa (R3c–O(I)–O(II), as above), plus evidence of non-reversibility, that is, persistence of a further orthorhombic phase O(III) after decompression. An orthorhombic—cubic transition was observed at 44.6 GPa using Raman scattering.[17]

A study of $PbTiO_3$ showed a number of structural phase transitions above 11 GPa.[18] Ahart[19] and Wu[20] showed the presence of a morphotropic phase boundary for $PbTiO_3$ as a function of pressure, with passage from tetragonal at low pressure to rhombohedral at high pressure, with an intermediate monoclinic phase. A second order transition was observed at 12.1 GPa, using Raman scattering.[21]

In La-doped PZT, $Pb_{(1-x)}La_x(Zr_{0.90}Ti_{0.10})_{1-x/4}O_3$ a ferroelectric to antiferroelectric phase transition occurred at ca. 100 MPa for $x = 0.03$ and 300 MPa for $x = 0.02$ at room temperature.[22] In $Pb_{0.99}(Zr_{0.95}Ti_{0.05})_{0.98}Nb_{0.02}O_3$, a transformation from ferroelectric to antiferroelectric commenced at 210 MPa at room temperature, with a volume difference of 0.8% between the two phases;[23] this volume difference provided the impetus for the phase transition. After unloading, the antiferroelectric structure persisted (74% by weight, as determined using structural analysis), showing considerable hysteresis; only after heating to 350 K was the ferroelectric phase fully restored.

Clearly, by comparing the ferroelectric–antiferroelectric phase transition in Zr-rich PZT, as above, we can draw analogues with the $BiFeO_3$–$PbTiO_3$ system reported here; both materials display (a) close vicinity to a crystallographic phase boundary and (b) a significant unit cell volume difference between the two crystallographic phases in each material, that is ferroelectric (R3c) and antiferroelectric (Pbam) in PZT and paramagnetic (P4mm) and antiferromagnetic (R3c) in $BiFeO_3$–$PbTiO_3$.

The motivation for the experiments presented here was to determine whether the application of moderate hydrostatic pressures could be used to induce a P4mm to R3c transition in $BiFeO_3$–$PbTiO_3$, the driving force being the volume difference between the two phases; this mechanism would differ significantly in nature from the pressure induced transitions for pure $BiFeO_3$ and $PbTiO_3$, or the electric field induced transition in relaxor ferroelectric single crystals.[24] We have shown previously that, at room temperature, the R3c phase displays antiferromagnetic ordering, whereas P4mm is paramagnetic.[9] One anticipates that a pressure induced transformation from para- to antiferromagnetic ordering would accompany the structural transition.

II. EXPERIMENTAL DETAILS

Single phase stoichiometric materials of $0.65BiFeO_3$–$0.35PbTiO_3$ and $0.7BiFeO_3$–$0.3PbTiO_3$ were prepared by conventional mixed oxide synthesis. The composition was set such that in the ABO_3 structure, $A = B = 1$. These two tetragonal materials were chosen, due to their proximity to the compositional phase boundary between P4mm and R3c. The precursor metal oxide powders (Aldrich, 99.9%) were milled in 2-propanol, dried, sieved, and calcined at 800 °C for 4 h. The resultant single phase was milled, dried, and sieved as before, this time with the addition of binder (1 w/w % Glascol HA40, Ciba). Green pellets were prepared 15 mm diameter × 20 mm high by pressing uniaxially at 50 MPa. The green pellets were subsequently isostatically pressed at 250 MPa, to further improve compaction.

Disintegrated powders were made by rapidly cooling these ceramic bodies from a temperature of 1100 °C, as reported in previous work.[9] The large stress induced by this process lead to disintegration of the ceramic into a powder. Neutron diffraction experiments revealed that magnetic ordering in the P4mm phase was absent at room temperature, in agreement with magnetic measurements by Zhu, which showed paramagnetism for tetragonal compositions.[5] The weight loss of the powder was monitored before and after sintering/disintegration and was found to be negligible (<0.1% by weight), suggesting that Bi_2O_3 and PbO loss was extremely low.

In-situ neutron diffraction measurements were conducted on the Pearl beamline located at the ISIS Facility, Rutherford Appleton Labs, UK. The Pearl time-of-flight neutron powder diffractometer is a high-flux instrument optimized for data collection from the Paris-Edinburgh (P-E) pressure cell.[25,26] In addition to the powder under study, a small Pb sphere (ca. 0.8 mm diameter) was included in the standard null-scattering TiZr gasket[27] for use as a pressure marker, along with a few drops of a 4:1 by volume mixture of perdeuterated methanol/ethanol pressure transmitting medium.[28]

Using the conventional collection mode of Pearl, data were collected using high resolution banks centred at 90°, corresponding to a d-spacing range of 0.3 to 4.15 Å. In order to allow for direct observation of the magnetic only peak expected at ca. 4.6 Å, the sample cradle was rotated and tilted at selected pressures, and the low angle detectors (centred at 30°) were employed. This configuration allowed for collection over a range in d-spacing of ca. 1 to 8.5 Å, albeit with poorer resolution and statistics, with significant contributions from the sample environment. Fortunately, Bragg peaks from the sample environment were absent above 2.85 Å, in the region of interest.

GSAS[29] (General Structure Analysis System) was used to refine the structural and magnetic model parameters using the observed diffraction data. The findings of our previous neutron diffraction measurements were used as a starting point for the models, with a paramagnetic P4mm cell for the tetragonal phase. In order to model the transformed magnetic structure, a unit cell of P1 symmetry populated using Fe ions with a B-site concentration of 0.7 or 0.65 was constrained to the R3c nuclear model.

A series of diffraction patterns were collected with increasing hydrostatic pressure. During the experiment, the position of the (200) Pb Bragg reflection at ca 2.5 Å was used as a guide to the pressure; upon refinement of the model, a more precise value was obtained from the Pb lattice parameter and equation of state.[30–33] These values were used as the abscissae in Figures 2–4.

X-ray diffraction as a function of temperature and subsequent structural refinement, were conducted using a P'Analytical X'Pert MPD (Almelo, the Netherlands) with associated HIGHSCORE PLUS software.

III. RESULTS AND DISCUSSION

A. Effect of applied pressure on structure

Figure 1 shows the results of a structural refinement of $0.7BiFeO_3$–$0.3PbTiO_3$ powder within the P-E cell at the initial sealing load of 7 ton, corresponding to a hydrostatic pressure ≈ 0. From Figure 1, it can be seen that the pattern contains contributions from a total of four phases, the most intense being from the P4mm tetragonal phase of $0.7BiFeO_3$–$0.3PbTiO_3$ and the Pb pressure marker. Weaker contributions are present due to tungsten carbide (WC) and Ni which originate from the anvils of the P-E cell. The lattice parameters (a = 3.813 and c = 4.534) are similar to reports in the literature for $0.7BiFeO_3$–$0.3PbTiO_3$ using x-ray diffraction[8] (a = 3.816 and c = 4.528).

For the purposes of the structural refinement, a number of constraints were imposed in order to prevent divergence. For example, one overall isotropic temperature factor was used universally across both ferroelectric models ($U_{ov} = U_{iso}$ (P4mm) = U_{iso} (R3c)) for all atoms. Additionally, the large A-site atoms were fixed at the origin. The atomic displacements of the B-site atoms were constrained to each other, within the same phase, and likewise the displacement of the oxygen atoms in the tetragonal phase. At zero pressure, $z_{Fe,Ti} = 0.05(2)$, $z_{O1,O2} = 0.17(7)$ and $U_{ISO} = 0.0179(2)$ Å^2 for $0.7BiFeO_3$–$0.3PbTiO_3$. The results of the refinement for 0.65 $BiFeO_3$–$0.35PbTiO_3$ are not shown here, but the same procedure was used as for $0.7BiFeO_3$–$0.3PbTiO_3$.

Figure 2 shows the effect of increasing hydrostatic pressure on the ferroelectric phase concentration; for both materials, there was a modification of the structure from P4mm to R3c. For $0.65BiFeO_3$–$0.35PbTiO_3$, transformation started at of 0.67 GPa and was completed by 0.88 GPa, whereas for

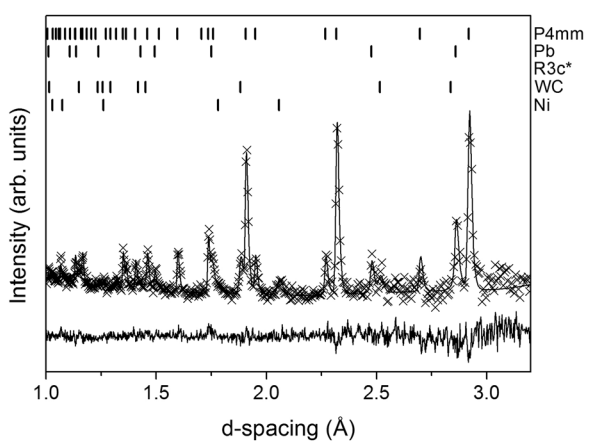

FIG. 1. Structural refinement for $0.7BiFeO_3$–$0.3PbTiO_3$ disintegrated powder at zero hydrostatic pressure within the P-E pressure cell. A number of data points have been removed to improve clarity. Collected data are shown by crosses, with a solid line for the refined model. The lower solid line shows the difference plot between the collected data and the model. $R_p = 0.057$ and $R_{wp} = 0.069$. *The R3c phase is absent at zero pressure.

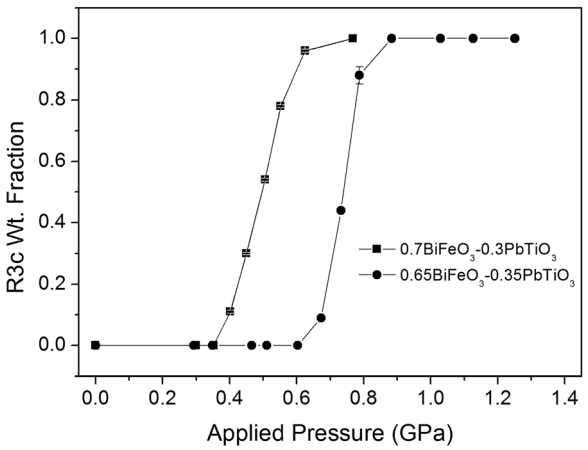

FIG. 2. Variation in weight fraction of R3c phase with increasing hydrostatic pressure for $0.65BiFeO_3$–$0.35PbTiO_3$ and $0.7BiFeO_3$–$0.3PbTiO_3$.

$0.7BiFeO_3$–$0.3PbTiO_3$, which is closer to the phase boundary, transformation proceeded at 0.4 GPa and was completed by 0.77 GPa. The transformation was not instantaneous, that is, a mixed phase region persisted over a significant pressure range. Note that the transformation proceeded through a mixed phase region and not via an intermediate phase, such as monoclinic or orthorhombic as observed in other systems.

The effect of pressure on the primitive unit cell volumes (1/6 volume for the R3c phase, the primitive cell, was used to allow for comparison) is plotted in Figure 3 for both materials. As one would expect, the unit cell volume decreased markedly as the pressure was increased. The P4mm phase always presents a far higher cell volume (ca. 4.9% for and $0.7BiFeO_3$–$0.3PbTiO_3$ and 3.9% for $0.65BiFeO_3$–$0.35PbTiO_3$), and therefore, a lower density than the R3c phase. It is this difference in volume that provides the driving force for the pressure induced phase transition, and this mechanism differs markedly from the $BiFeO_3$ and $PbTiO_3$ end members reported earlier.

Figure 4 shows the variation in spontaneous strain for both P4mm and R3c phases as a function of hydrostatic pressure, calculated as (c-a)/a for the P4mm and tan(90-α), in pseudocubic space,[34] for the R3c phase. If the low pressure

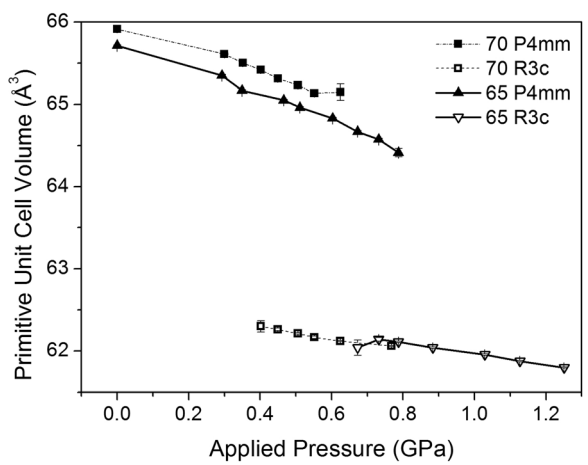

FIG. 3. Variation in unit cell volume for $0.65BiFeO_3$–$0.35PbTiO_3$ and $0.7BiFeO_3$–$0.3PbTiO_3$ as a function of applied hydrostatic pressure.

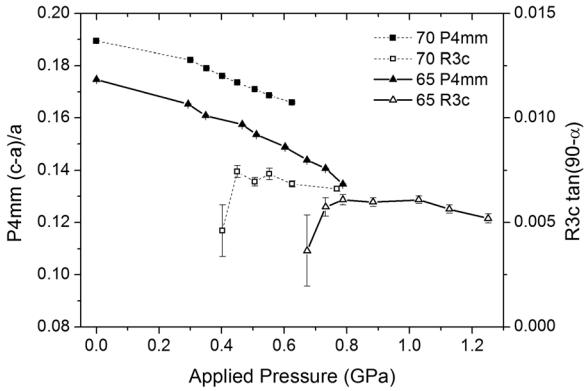

FIG. 4. Effect of applied hydrostatic pressure on spontaneous strain for $0.65BiFeO_3$–$0.35PbTiO_3$ and $0.7BiFeO_3$–$0.3PbTiO_3$, calculated as (c-a)/a for P4mm and tan(90 -α) for R3c, using a pseudo-cubic setting.

data are ignored for the R3c phase (due to large error bars), a clear relationship can be shown between a decrease in ferroelectric spontaneous strain and increasing pressure in both P4mm and R3c phases. An interpolation of this data would suggest that eventually, with increasing pressure, the spontaneous strain may reach zero, and ferroelectricity would be lost, as observed in other systems, such as $BaTiO_3$[35] and PZT.[36,37] For the $BiFeO_3$ and $PbTiO_3$ end members, a decrease in spontaneous strain is also observed as the pressure is increased.

Figure 5 shows the outcome from the structural refinement of the disintegrated $0.7BiFeO_3$–$0.3PbTiO_3$ powder at a pressure of 0.77 GPa, which shows transformation to 100% R3c phase. The 113 reflection, which results from both oxygen octahedral tilting and antiferromagnetic ordering is marked and discussed later.

Upon unloading the pressure cell, after completion of the experiment, it was observed that the transformed R3c phase persisted in the composition $0.7BiFeO_3$–$0.3PbTiO_3$, that is, the R3c did not revert to the initial P4mm. Data were collected using Polaris (ISIS), for the same sample in a glass capillary, 400 h after the Pearl experiment, which again showed 100% R3c phase (discussed later in reference to magnetic ordering). This strongly suggests that a potential energy barrier exists, indicating a first order transition due to the difference in density of the two phases. This energy barrier must be overcome with pressure to affect a transformation and prevents reversal upon removal of the pressure, even after a significant period of time had elapsed. This irreversibility has been observed in other systems, as highlighted in the introduction. To the contrary, the composition $0.65BiFeO_3$–$0.35PbTiO_3$ reverted back to the P4mm phase on removal of the pressure.

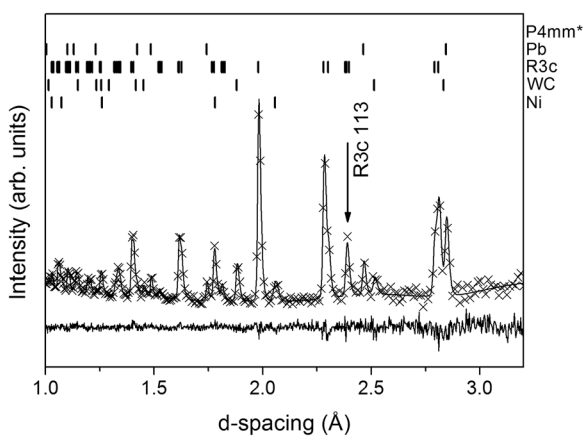

FIG. 5. Structural refinement for the $0.7BiFeO_3$–$0.3PbTiO_3$ disintegrated powder after transformation to R3c phase at a pressure of 0.77 GPa, cf. Figure 1. The arrow at ca. 2.4 Å denotes the R3c 113 peak, which comprises both nuclear and magnetic contributions. *: Once transformed, the P4mm phase is absent.

B. Effect of hydrostatic pressure on magnetic ordering

In order to study the magnetic only Bragg peak at ca. 4.6 Å, the configuration of Pearl was modified at selected pressures. In order to further refine the magnetic moment on the Fe^{3+} ions, the structural and magnetic models generated in the previous section were used (and left unaltered) with the data collected in this configuration; at this point, only refinement to the Fe^{3+} moment was permitted. The outcome of this procedure is shown graphically in Figure 6, using collection times of 4 h per measurement, more than double that required for collection using the 90° detectors. The peaks are extremely broad, and below 3 Å, dominated by the pressure cell gaskets.

Figure 6 shows a pressure induced transformation from P4mm to R3c, and with it a transformation from para- to antiferromagnetic ordering, for both materials. The position of the P4mm (001) and the R3c magnetic (101) and (003) peaks are in similar but significantly different positions of

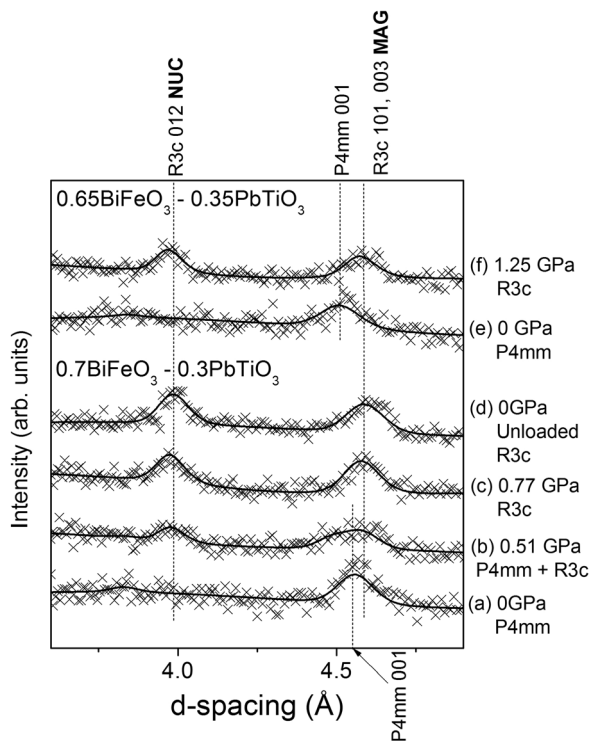

FIG. 6. Diffraction data of $0.7BiFeO_3$–$0.3PbTiO_3$ (a)–(d) and $0.65BiFeO_3$–$0.35PbTiO_3$ (e)–(f) collected using low-angle bank on Pearl. The pressures and phase assemblage are labeled.

4.535 and 4.587 Å, respectively, at zero pressure for $0.7BiFeO_3$–$0.3PbTiO_3$, Figures 6(a) and 6(d). A large broad peak can be observed at a pressure 0.51 GPa for $0.7BiFeO_3$–$0.3PbTiO_3$ (Figure 6(b)) for these positions, due to coexistence of the P4mm structural and R3c magnetic peaks, 54 wt. % R3c phase. To recap, the peak at 4.535 Å in the lower trace is nuclear, whereby in Figures 6(c) and 6(d) at ca 4.6 Å (the position clearly changes as a function of pressure), it is entirely magnetic.

As mentioned previously, the $0.7BiFeO_3$–$0.3PbTiO_3$ sample was analyzed 400 h later in a glass capillary at ambient temperature and pressure using Polaris at ISIS. Polaris can access an extremely wide d-spacing range, from 0.2 to 21 Å. A magnetic and structural refinement performed using data from the low angle (A-bank, low resolution) and back-scattered (C-bank, high resolution) detectors are shown in Figure 7. Using this beamline, we can show unequivocally that transformation from P4mm to R3c has occurred in $0.7BiFeO_3$–$0.3PbTiO_3$, and with it a transformation from para- to antiferromagnetic ordering; the Bragg peak at 4.6 Å is due entirely to G-type antiferromagnetic ordering and has no nuclear contributions. The transformed R3c structure at ambient pressure provides strong supporting evidence, in conjunction with Fig. 6, that the high pressure R3c phase is also antiferromagnetic, with G-type ordering.

Due to the low amount of powder measured (ca. 50 mg, ideally > 5 g required) some residual peaks, with the strongest signals at 4.26, 2.93, and 1.91 Å. From a search of these peaks in the ICDD database (International Centre for Diffraction Data), we have been unable to identify the nature of this material. These peaks were not observed using powder x-ray diffraction.

The outcome of the refinement relating to Figure 7 is shown in Table I. Using Polaris, without the contributions of a pressure cell, it is possible to refine separate temperature factors for the A-, B-, and O sites.

Table II shows a summary of the findings with respect to the inclusion of the low angle bank on Pearl plus the data collection *ex-situ* using Polaris for $0.7BiFeO_3$–$0.3PbTiO_3$. It can be seen that the once formed, the antiferromagnetic ordering in the R3c phase persists, with a moment of between 2.7 and 3 μ_B.

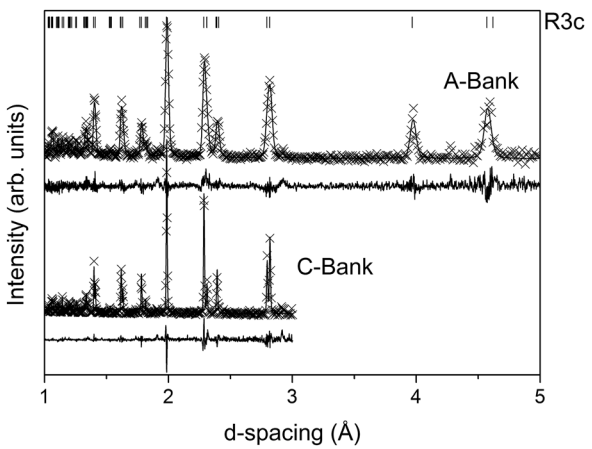

FIG. 7. Diffraction data of $0.7BiFeO_3$–$0.3PbTiO_3$ collected using Polaris, 400 h after pressure experiment on Pearl. Data are presented from the A-bank (high d-spacing, low resolution) and C-bank (up to 3 Å d-spacing, high resolution). The tick-marks for R3c phase are shown at the top of the figure.

TABLE I. Structural and magnetic refinement for $0.7BiFeO_3$–$0.3PbTiO_3$ collected on Polaris, 400 h after pressure experiment on Pearl. The residuals are cumulative from the refinement of both A and C banks.

Parameter	$0.7BiFeO_3$-$0.3PbTiO_3$ R3c
a/Å	5.5898(6)
c/Å	13.858(5)
$z_{Bi,Pb}$	0
$z_{Fe,Ti}$	0.227(9)
x_O	0.462(9)
y_O	0.012(4)
z_O	0.961(1)
$U_{ISO\ (Pb,Bi)}/Å^2$	0.018(2)
$U_{ISO\ (Fe,Ti)}/Å^2$	0.004(6)
$U_{ISO\ (O)}/Å^2$	0.013(6)
μ_{Fe}/μ_B	2.9(5)
R_p	0.0828
R_{wp}	0.1439

For the material $0.65BiFeO_3$–$0.35PbTiO_3$, a slightly lower magnetic moment of 2.3(8) μ_B was observed at 1.25 GPa, as anticipated; the introduction of more Ti dilutes and disrupts the exchange between the antiferromagnetically ordered Fe.

C. X-ray diffraction of transformed powder

Six months after the experiments using Pearl and Polaris, the same sample of $0.7BiFeO_3$–$0.3PbTiO_3$ was analyzed using conventional laboratory XRD. Rietveld analysis of the powder showed the presence of a small quantity (7 wt. %) of P4mm phase. Diffraction patterns were collected with increasing temperature *in-situ* using a hot stage, the results of which are shown in Figure 8.

Upon heating, the concentration of the transformed R3c phase rapidly diminished and reached a steady value of between 6 and 7 wt. % at 310 °C and above. As the temperature was increased further, transformation to cubic occurred by 640 °C which is commensurate with the findings of previous groups.[8] Interestingly, at 590 °C, a mixed phase region consisting of the tetragonal P4mm and cubic (Pm-3 m) occurs, prior to total transformation, suggesting that the R3c phase transformed to cubic more readily that P4mm. After cooling back to room temperature, the R3c was only partially restored and a small concentration of P4mm (5%) persisted.

The low temperatures required to initiate the transformation from predominantly R3c back to P4mm (100–200 °C)

TABLE II. Phase fraction and refined moment for $0.7BiFeO_3$–$0.3PbTiO_3$ disintegrated powder prior to, during and after transformation.

Load/GPa	Note	Wt. fraction, R3c	Refined moment/Fe (R3c), μ_B
0	Start of experiment	0	0
0.51	Partial transformation	0.54	2.(8)
0.77	Complete transformation to R3c	1	2.8(3)
0	Removal of pressure	1	2.7(1)
0	After 400 h	1	2.9(5)

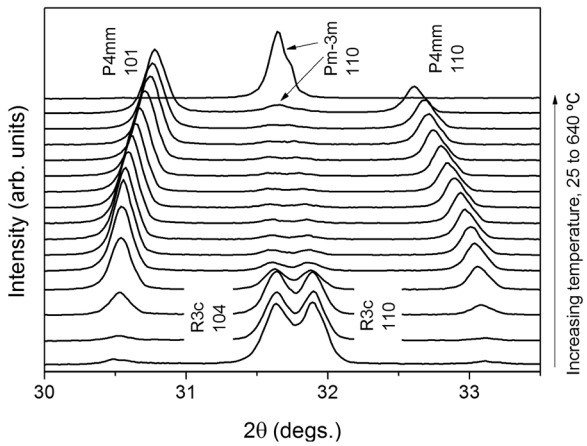

FIG. 8. X-ray diffraction patterns for $0.7BiFeO_3$–$0.3PbTiO_3$ disintegrated powder, transformed to R3c in Pearl pressure cell. Above 100 °C the concentration R3c phase rapidly decreases. The range shown in degrees 2θ corresponds to a range in d-spacing of 2.67–2.98 Å. Note that the doublet observed for the Pm-3 m peak is due to Cu $K\alpha_1/K\alpha_2$ radiation.

are far lower than either the antiferromagnetic Néel temperature (287 °C)[38] or ferroelectric Curie point (632 °C)[8] for this composition. Although we are unable to tell (using x-ray diffraction), we assume that the transformation back to predominantly tetragonal phase is associated with a loss of antiferromagnetic order.

IV. DISCUSSION AND CONCLUSIONS

At ambient temperature and pressure, the compositions $0.7BiFeO_3$–$0.3PbTiO_3$ and $0.65BiFeO_3$–$0.35PbTiO_3$ possess tetragonal symmetry, P4mm, with paramagnetic ordering. With the application of moderate hydrostatic pressures (<0.9 GPa), P4mm phase readily transforms to rhombohedral symmetry, R3c, at room temperature. We are able to show that a transformation from para- to G-type antiferromagnetic ordering accompanies this structural transition for both compositions. To our knowledge, a pressure induced para- to antiferromagnetic transition is unique in the literature; many systems show the reverse, that is, loss of magnetic ordering under high pressure.

The pressures required to affect a phase transition are clearly far lower than that of the $BiFeO_3$ or $PbTiO_3$ end members; recall that $BiFeO_3$ transforms from its ambient R3c structure to orthorhombic at 2.5 GPa[15] and $PbTiO_3$ from P4mm to monoclinic at 11 GPa.[19] The driving force for the phase transition reported here is due to the large volume difference between R3c and P4mm phases of 4%-5%, plus the locality of the two tetragonal compositions to the phase boundary between tetragonal and rhombohedral phase. The stimulus for the pressure induced transition is clearly the same as that observed in Zr-rich PZT, as discussed previously, where transformation from R3c to Pbam occurs at 210 MPa, as a result of the close vicinity of the antiferroelectric–ferroelectric phase transition, and the ca. 0.8% volume difference between the two phases.

The two materials studied here do behave differently to each other, however; upon removal of external pressure, the crystal structure reverts back from R3c to P4mm for $0.65BiFeO_3$–$0.35PbTiO_3$ and magnetic ordering is lost. For $0.7BiFeO_3$–$0.3PbTiO_3$, the R3c phase persists when the pressure is removed, and antiferromagnetic ordering remains. The transformed rhombohedral magnetic structure in $0.7BiFeO_3$–$0.3PbTiO_3$ was stable over a significant period of time; 400 h later, neutron diffraction of the same powder sample yielded identical results, with 100% R3c, antiferromagnetic phase. Using conventional lab XRD after 6 months showed partial reversal had occurred, with 7% P4mm. The original P4mm phase was readily restored with moderate temperatures, far below that of either the antiferromagnetic Néel temperature or the ferroelectric Curie point. Again, an analogy can be drawn with Zr-rich PZT whereby, after decompression to ambient pressure, 74% of the antiferroelectric phase persisted, and an increase in temperature to ca. 75 °C was required to fully restore the ferroelectric phase. Hysteresis was observed in a number of other materials, as discussed in the introduction.

There is also a distinction in (a) the pressure required to affect the structural and magnetic phase change and (b) the range in pressure across which the transformation occurs. $0.7BiFeO_3$–$0.3PbTiO_3$ transforms far more readily and over a larger pressure range than $0.65BiFeO_3$–$0.35PbTiO_3$. One assumes that a higher pressure is required to affect transformation in $0.65BiFeO_3$–$0.35PbTiO_3$ as it is further removed from the R3c-P4mm phase boundary, and the volume difference between the P4mm and R3c phase is lower.

There are a number of mechanisms which may result in a mixed phase at intermediate pressures, such as small local deviations in chemistry, or generation of hoop stresses, where the core of a grain experiences a lower pressure than encountered by the skin.

[1]C. Michel, J.-M. Moreau, G. D. Achenbach, R. Gerson, and W. J. James, Solid State Commun. **7**, 701 (1969).
[2]F. Kubel and H. Schmid, Acta Crystallogr **46**, 698 (1990).
[3]G. Catalan and J. F. Scott, Adv. Mater. **21**, 2463 (2009).
[4]S. A. Fedulov, P. B. Ladyzhinskii, I. L. Pyatigorskaya, and Y. N. Venevtsev, Sov. Phys. Solid State **6**(2), 375 (1964).
[5]W.-M. Zhu, H.-Y. Guo, and Z.-G. Ye, Phys. Rev. B **78**, 014401 (2008).
[6]T. P. Comyn, T. Stevenson, and A. J. Bell, J. Phys. IV **128**, 13 (2005).
[7]T. Smith, G. D. Achenbach, R. Gerson, and W. J. James, J. Appl. Phys. **39**(1), 70 (1968).
[8]V. V. S. S. Sai Sunder, A. Halliyal, and A. M. Umarji, J. Mater. Res. **10**, 1301 (1995).
[9]T. P. Comyn, T. Stevenson, M. Al-Jawad, S. L. Turner, R. I. Smith, W. G. Marshall, A. J. Bell, and R. Cywinski, Appl. Phys. Letts. **93**, 232901 (2008).
[10]S. Bhattacharjee, V. Pandey, R. K. Kotnala, and D. Pandey, Appl. Phys. Lett. **94**, 012906 (2009).
[11]T. P. Comyn, T. Stevenson, M. Al-Jawad, S. L. Turner, R. I. Smith, A. J. Bell, and R. Cywinski, J. Appl. Phys. **105**, 094108 (2009).
[12]R. Haumont, J. Kriesel, and P. Bouvier, Phase Transitions **79**(12), 1043 (2006).
[13]R. Haumont, P. Bouvier, A. Pashkin, K. Rabia, S. Frank, B. Dkhil, W. A. Crichton, C. A. Kuntscher, and J. Kreisel, Phys. Rev. B **79**, 184110 (2009).
[14]A. Pashkin, K. Rabia, S. Frank, C. A. Kuntscher, R. Haumont, R. Saint-Martin, and J. Kreisel, Condens. Matter; e-print arXiv:0712.0736 (2007).
[15]A. G. Gavriliuk, V. V. Struzhkin, I. S. Lyubutin, M. Y. Hu, and H. K. Mao, JETP Lett. **82**(4), 224 (2005).
[16]A. A. Belik, H. Yusa, N. Hirao, Y. Ohishi, and E. Takayama-Muromachi, Chem. Mater. **21**, 3400–3405 (2009).
[17]Y. Yang, L. G. Bai, K. Zhu, Y. L. Liu, S. Jiang, J. Liu, J. Chen, and X. R. Xing, J. Phys.: Condens. Matter. **21**, 385901 (2009).
[18]P.-E. Janolin, P. Bouvier, J. Kreisel, P. A. Thomas, I. A. Kornev, L. Bellaiche, W. Crichton, M. Hanfland, and B. Dkhil, Phys. Rev. Lett. **101**, 237601 (2008).
[19]M. Ahart, M. Somayazulu, R. E. Cohen, P. Ganesh, P. Dera, H.-K. Mao, R. J. Hemley, Y. Ren, P. Liermann, and Z. Wu, Nature **451**, 545 (2008).

[20]Z. Wu and R. E. Cohen, Phys. Rev. Lett. **95**, 037601 (2005).
[21]J. A. Sanjurjo, E. López-Cruz, and G. Burns, Phys. Rev. B **28**, 7260 (1983).
[22]A. Peláiz-Barranco and D. A. Hall, IEEE Trans. Ultrason. Ferroelectr. Freq. Control **56**(9), 1785 (2009).
[23]M. Avdeev, J. D. Jorgensen, S. Short, G. A. Samara, E. L. Venturini, P. Yang, and B. Morosin, Phys. Rev. B **73**, 064105, (2006).
[24]S.-E. Park and T. R. Shrout, J. Appl. Phys. **82**(4), 1804 (1997).
[25]R. J. Nelmes, J. S. Loveday, R. M. Wilson, J. M. Besson, S. Klotz, G. Hamel, and S. Hull, Trans. Am. Crystallogr. Assoc. **29**, 19 (1994).
[26]J. M. Besson, R. J. Nelmes, G. Hamel, J. S. Loveday, G. Weill, and S. Hull, Physica B **180**, 907 (1992).
[27]W. G. Marshall and D. J. Francis, J. Appl. Crystallogr. **35**, 122 (2002).
[28]D. R. Allan, W. G. Marshall, and C. R. Pulham, Am. Mineral. **92**, 1018 (2007).
[29]A. C. Larson and R. B. Von Dreele, *General Structure Analysis System (GSAS)* (Los Alamos National Laboratory Report LAUR, 2004), pp. 86–748.
[30]D. Fortes, Ph.D. dissertation, University College, University of London, 2004.
[31]Z. Kuznetsov, V. Dmitriev, L. Dubrovinsky, V. Prakapenka, and H.-P. Weber, Solid State Commun. **122**, 125 (2002).
[32]R. A. Miller and D. E. Schuele, J. Phys. Chem. Solids **30**, 589 (1969).
[33]D. L. Waldorf and G. A. Alers, J. Appl. Phys. **33**, 3266 (1962).
[34]J.-M. Moreau, C. Michel, R. Gerson, and W. J. James, Acta Crystallogr. **26**, 1425 (1970).
[35]Ph. Pruzan, D. Gourdain, J. C. Chervin, B. Canny, B. Couzinet, and M. Hanfland, Solid State Commun. **123**, 21 (2002).
[36]J. Rouquette, V. Bornand, J. Haines, Ph. Papet, and F. Gorelli, Integr. Ferroelectr. **48**(1), 53 (2002).
[37]J. Rouquette, J. Haines, G. Fraysse, A. Al-Zein, V. Bornand, M. Pintard, Ph. Papet, S. Hull, and F. A. Gorelli, Inorg. Chem. **47**, 9898 (2008).
[38]T. Stevenson, T. P. Comyn, A. J. Bell, and R. Cywinski, in *Proceedings of the 16th IEEE ISAF*, 27-31 May 2007 (Nara, Japan, 2007), Vol. 1 and 2, p. 421.